Numerical explorations of solvent borne adhesives: a lattice-based approach to morphology formation

Numerical explorations of solvent borne adhesives: a lattice-based approach to morphology formation

OPEN ACCESS
IOP Publishing
Modelling and Simulation in Materials Science and Engineering
Modelling Simul. Mater. Sci. Eng. **31** (2023) 075005 (14pp) https://doi.org/10.1088/1361-651X/acee5b

Numerical explorations of solvent borne adhesives: a lattice-based approach to morphology formation

V Cecilia Erik Kronberg[1], Stela Andrea Muntean[2], Nils Hendrik Kröger[3] and Adrian Muntean[4,*]

[1] Department of Mathematics and Computer Science, Eindhoven University of Technology, Eindhoven, The Netherlands
[2] Department of Engineering and Physics, Karlstad University, Karlstad, Sweden
[3] tesa SE, Norderstedt, Germany
[4] Department of Mathematics and Computer Science, Karlstad University, Karlstad, Sweden

E-mail: adrian.muntean@kau.se

Received 28 May 2023; revised 14 July 2023
Accepted for publication 25 July 2023
Published 25 August 2023

Abstract

The internal structure of adhesive tapes determines the effective mechanical properties. This holds true especially for blended systems, here consisting of acrylate and rubber phases. In this note, we propose a lattice-based model to study numerically the formation of internal morphologies within a four-component mixture (of discrete particles) where the solvent components evaporate. Mimicking numerically the interaction between rubber, acrylate, and two different types of solvents, relevant for the technology of adhesive tapes, we aim to obtain realistic distributions of rubber ball-shaped morphologies—they play a key role in the overall functionality of those special adhesives. Our model incorporates the evaporation of both solvents and allows for tuning the strength of two essentially different solvent–solute interactions and of the temperature of the system.

* Author to whom any correspondence should be addressed.

Keywords: phase separation, adhesive tapes, rubber morphologies, lattice-based simulations

(Some figures may appear in colour only in the online journal)

1. Introduction

An adhesive is usually a thin flexible layer that is applied on the boundary of objects aiming to join them together via an adhesive bonding process. The adhesive bonding is a complex process and its efficiency is directly influenced by the internal structure (here referred to as 'morphology') of the layer. In this note, we focus our discussion on acrylic pressure sensitive adhesives (PSAs), as they are one of the most important and widely used classes of adhesives. They have applications ranging from standard tapes and labels to special protective films (sealing, e.g. against oxidation or solar radiation). We refer the reader to [MMM21] for a recent review of the classification of adhesive tapes and their applications. One of many possibilities of enhancing the properties of PSAs is blending the acrylic base formulation with rubber. Here, our main interest lies in understanding the phase separation properties of a highly interacting multi-component mixture that is prepared in the production phase of solvent-borne adhesives. Specifically, and as a simplification, we investigate a combination of four species (acrylate, rubber, and two distinct solvents), allowing for the possibility of evaporating the two solvents[5]. A typical experimental picture we have in mind for this setting is shown in figure 1. For this precise case, the two solvents are ethylacetate (solvent 1) and benzine (solvent 2), but the overall picture should be perceived in a generic way.

The main question we pose here is twofold:

> What influence does the temperature during the evaporation process have on the distribution of the rubber phase and on the dispersion of the two solvents during the evaporation process?

To address this question, we propose a study based on a stochastic lattice-type model that describes the initiation phase of the mixture, the actual dynamics leading to morphology formation (multi-component diffusion, interaction, and evaporation), and finally, a calibration phase—referred here as migration phase. In this last phase, the obtained morphologies stabilize their terminal shape and any remaining solvent is allowed to disperse more evenly throughout the system with a switched-off evaporation process. Within this frame, we apply the methodology that we developed for a numerical investigation of morphology formation as it occurs in the case of organic solar cells (OSCs); see our recent work reported in [CCM+19, MKC+22, SKM+23].

The main common feature of both OSC and PSA systems is that the phase separation property arises during the interplay of the diffusion transport of a highly-interacting mixture of

[5] In industrial formulations additional ingredients are added like tackifying resins, wetting agents, anti-aging agents, plasticizers and more.

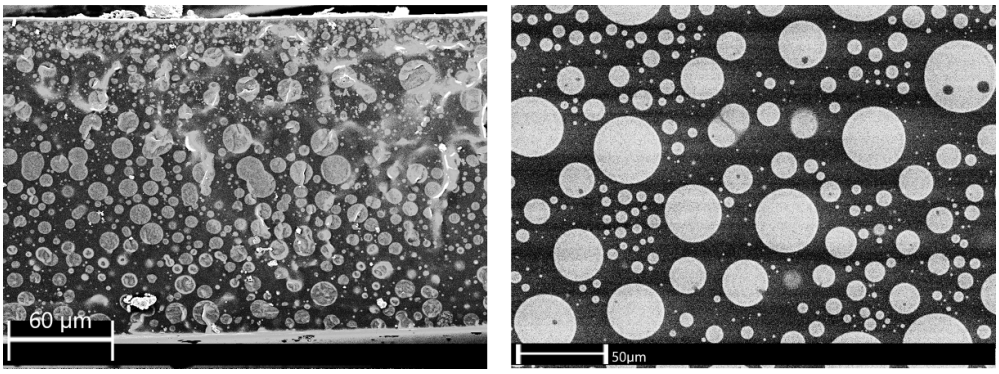

Figure 1. Left panel: side view on the thin film. Right panel: top view on the thin film. The ball-type structures are rubber parts; within an acrylate matrix. The two solvents, ethylacetate and benzine, will evaporate fully, if the process is not stopped, and are indistinguishable in the experimental pictures. We see that multiple rubber disks coalesce to form larger ones, much like in our simulation.

polymers and solvent, with the solvent evaporating until a certain mass fraction is reached. Obviously, the type of polymers and choices of solvents are very different in PSA compared to OSC, but the essential conceptual difference relies on the fact that for PSA systems, the temperature (and eventually also temperature gradients) play a prominent role in the formation of the final film and moreover, more solvents can be present in the mixture. Our description is stochastic, it holds at a discrete level (the lattice), and handles the time evolution and spatial localization of all the mass fractions in the mixture. On the other hand, as we are tracing only the evolution of mass fractions, no information about the transfer of momentum can be captured at this level. Consequently, neither fluid dynamics effects nor macroscopic mechanical responses of the film can be explored within our framework. To this end, conceptually different approaches need to be taken; we refer the reader to [SEP+21] (adhesive materials and friction), [RKZ+23] (dynamical adhesive contact in visco-elastic materials) and [EBS+20] (conservation of historical heritage) for remotely related situations where linear momentum information is handled computationally without aiming to capture insights in the dynamics of the phase separation.

The paper is organized as follows. In section 2, we describe the lattice model, and in section 3, we show our simulation results and then discuss their relevance. The conclusion of this study as well as an outlook of further possible questions to be investigated in this setting are the subject of section 4.

2. The lattice-based model

In this section, we give the details of our lattice-based model and describe the algorithm used to perform the simulations. The implementation of the algorithm is done in MATLAB and is publicly available at https://github.com/vcekron/solventAdhesive.

2.1. The lattice

Consider a rectangular two-dimensional lattice $\Lambda = \{1,\dots,L_1\} \times \{1,\dots,L_2\}$, where $L_1 \geqslant L_2$. An element of Λ is called a *site*. Associated with each site are two *bonds*—one horizontal

Table 1. List of the mixture components with their coloring.

Species	Component	Color
1	Acrylate	Blue
2	Rubber	Yellow
3	Ethylacetate	Red
4	Benzine	Green

and one vertical—connecting each site to two neighboring sites. The sites are populated by a species variable $\sigma \in \{1,2,3,4\}$, where the meaning of each species variable is explained in table 1, where the 'color' property refers to the colors in the figures presented in the results section; see section 3.

2.2. The interaction matrix

The interaction between two neighboring sites depends on the two species—captured in the interaction matrix, denoted J,

$$J := \begin{pmatrix} J_{11} & J_{12} & J_{13} & J_{14} \\ J_{21} & J_{22} & J_{23} & J_{24} \\ J_{31} & J_{32} & J_{33} & J_{34} \\ J_{41} & J_{42} & J_{43} & J_{44} \end{pmatrix}, \tag{1}$$

which incorporates a few specific features regarding the way the components of the mixture interact with each other.

Besides the symmetry of the interaction matrix (compare [Han70]), we impose the following additional constraints on the entries of J, namely $J_{11} = J_{33} = J_{44} = 0$ (no self interaction for the acrylate and the two solvents), $J_{22} \ll 0$ (strong self-attraction for the rubber), $J_{34} > 0$ (the two solvents repel each other), $J_{24} > 0$ (rubber slightly repels solvent 2), $J_{23} > 0$ (rubber strongly repels solvent 1, which instead is less repelled by acrylate), and $J_{12} \gg 0$ (rubber and acrylate strongly repel each other). Furthermore, we only look to the case $J_{13} < J_{23}$ (solvent 1 repels acrylate more than it repels rubber). In this study, we have fixed the interaction matrix to be

$$J := \begin{pmatrix} 0 & 6 & 0.5 & 1.5 \\ 6 & -4 & 1 & 0.5 \\ 0.5 & 1 & 0 & 0.75 \\ 1.5 & 0.5 & 0.75 & 0 \end{pmatrix}, \tag{2}$$

in accordance with the description above, i.e. each of the entries in the interaction matrix describes the desired pairwise repulsion (positive sign) or attraction (negative sign) among the mixture components. The numerical values chosen in (2) indicate the relative strengths of the pairwise interactions. In this work, the interaction matrix components are not obtained via well-established lower scale physical theories, but are suitably chosen based on insights from the robustness study performed in [CCM+19] for the case of a ternary mixture driven by the same dynamics; see figures 4–9. in *loc. cit.* as well as the corresponding discussion. More accurate values could be obtained e.g. by calculating the enthalpy of mixing via molecular dynamics simulations of the molecules involved, as shown in [LGLM99, YHG+18].

Due to the importance of this interaction matrix with respect to the output of our four component mixture driven by the same dynamics, we chose to pay special attention to one of the

interaction parameters—J_{22}—the only attraction mechanism in the matrix. We vary this parameter and trace the corresponding effects; the results are shown in the appendix. We focus on J_{22} here since it also relates to the stability of the rubber (yellow) phase, which is one of the critical elements in PSA systems. A full parameter study with respect to the matrix J is outside of the scope of this paper.

2.3. The Hamiltonian

To simulate the dynamics of the lattice system, we let $\mathcal{H}$ represent the Hamiltonian associated with our system, i.e.

$$\mathcal{H} := \sum_{\langle i,j \rangle} J_{\sigma_i,\sigma_j}, \tag{3}$$

where the sum is carried out over nearest-neighbors, while J_{σ_i,σ_j} represents the components of J in equation (2). The energy difference between two configurations is then

$$\Delta E := \mathcal{H}^{\text{proposed}} - \mathcal{H}^{\text{current}}. \tag{4}$$

Here, the upper index 'current' of $\mathcal{H}$ refers to the evaluation of the Hamiltonian on the current configuration, while the upper index 'proposed' points out the evaluation of the Hamiltonian for the proposed configuration, where two sites have switched position.

Furthermore, let $\beta > 0$ be the inverse temperature, i.e. smaller β is associated with a higher temperature, and vice versa. The precise choice of β is essential in the fifth step of the Metropolis algorithm explained next.

2.4. The Metropolis algorithm

The evolution of our system is governed by the well-known Metropolis algorithm, which allows us to approximate the complex dynamics of the real system using five simple steps:

(1) pseudo-randomly select a *site* on Λ,
(2) pseudo-randomly select a *bond* associated with the site (vertical or horizontal),
(3) propose to switch the two spins occupying the bonded sites,
(4) evaluate the energy difference, ΔE from equation (4), associated with the switch,
(5) accept the proposed move with probability 1 if $\Delta E < 0$ and $\exp(-\beta \Delta E)$ otherwise.

It is not difficult to see that at a higher temperature, i.e. a smaller β will lead to more proposed moves being accepted in the Metropolis algorithm.

Correspondingly, higher values of β lead to colder systems, thus inhibiting large phase-separated domains from forming.

The boundary conditions depend on the stage of the simulation and on the species of the selected sites. In particular, our dynamics consist of three stages:

(1) the disks formation stage,
(2) the evaporation stage,
(3) the migration stage.

The first stage exists to provide a suitable starting point for the full simulation by using a reduced interaction matrix where only the rubber–rubber (yellow–yellow) interaction is switched on, i.e.

$$J_{\text{disks}} = \begin{pmatrix} 0 & 0 & 0 & 0 \\ 0 & -4 & 0 & 0 \\ 0 & 0 & 0 & 0 \\ 0 & 0 & 0 & 0 \end{pmatrix}. \tag{5}$$

This stage thus allows the rubber phase to aggregate before the full dynamics are switched on. Since this is an initialization stage, periodic boundary conditions are enforced during the disks formation stage.

The evaporation stage is then reached, during which the full dynamics are activated, and solvent sites are allowed to evaporate from the top boundary. This means that the full J from equation (2) is used and if a site at the top boundary is picked,

(1) the move is rejected (if the site is occupied by species 1 or 2 and the bond is vertical), or
(2) the spin at the site is replaced by a spin of species 1 (if the site is occupied by species 3 or 4). We call this operation *evaporation*, since it applies to the solvents.

Note that while we consider this the analog to the physical process of evaporation, care must be taken when comparing the two. In fact, due to the way our model is constructed, the lattice Λ is more accurately considered as a slice of a larger bulk material, so that the top boundary of Λ exists deep in the bulk material, and the 'evaporation' should be considered as a rapid a mass-exchange with an infinite reservoir[6]. Furthermore, both solvents respect here the same type of evaporation rule[7]. However, it is worth noting that the two solvents are expected to arrive very differently to the evaporation boundary as they undergo very different types and strengths of interaction with the mixture components they meet on the way. We will investigate in future works other options to model the solvent evaporation in the context of particle-based lattice models.

The left and right boundaries are periodic for every species during all stages. We end the evaporation stage when 10% total solvent remains in the system. There are many different valid stopping criteria, but either one is in some sense arbitrary, since the system is inherently dynamic. Our stopping criterion was chosen taken simulation time into account, whilst remaining physically relevant.

Finally, the migration stage is reached, during which time the full J is still used, but periodic boundary conditions are enforced for every species at every boundary. This stage, which can also be considered a terminal stage, was introduced to allow the solvent to migrate throughout the lattice.

It is beyond the scope of this work to enter into the technical details behind the Markov chain Monte Carlo method and the Metropolis algorithm. Instead, we refer the reader to, for instance, [OMIK99, CMv19] or the textbook [MGNR12].

3. Simulation results

This section shows the time evolution of the systems with a focus on two effects: the addition of the so-called disks formation stage and varying the system temperature. For further insight

[6] In particular, this means that looking at the solvent's behavior close to the evaporation surface we cannot account in the current description for the corresponding vapor pressures, boiling points, and local surface reaction behavior.

[7] We proceed in this way for our convenience. We can though extend the setting to include different probabilities of escape for each of the solvents. We do not do this here as it brings the attention away from our main interest—the morphology formation.

into the dynamics of the system, please see the movies of these simulations publicly available at https://github.com/vcekron/solventAdhesive.

Each simulation uses the following reference parameters: $L_1 = 256$, $L_2 = 128$, relative initial volume fractions $C_1 = 0.40$ and $C_2 = 0.15$, with the remaining 45% of the lattice sites being solvents with relative probabilities $P_3 = 0.7$ and $P_4 = 0.3$, so that their volume fractions are $C_3 = 0.315$ and $C_4 = 0.135$.

3.1. The disks formation stage

In order to study the effect of varying lengths of the disks formation stage for fixed temperature, consider figure 2.

Here, the same initial system was used for all three cases (top row). In the second row, the disks formation stage was carried out for zero iterations (first column), 10^8 iterations (second column; approximately $3 \cdot 10^3$ Monte Carlo steps (MCS)) and 10^9 iterations (third column; approximately $3 \cdot 10^4$ MCS). As was mentioned before, during the disks formation stage, only the rubber–rubber (yellow–yellow) interaction is switched on, and periodic boundary conditions are enforced everywhere without evaporation of the solvents. Once the disks formation stage is over, the full dynamics, including solvents evaporation from the top row, are switched on and the system is allowed to evolve. This evolution can be seen in consecutive rows after the second one, with snapshots at each 10% reduction in the total amount of solvent present in the system. Once the amount of solvent had reduced to 10% of the lattice sites (second to last row), the full dynamics were switched off and the so-called migration stage started. This stage lasted for 10^8 iterations. During this stage, periodic boundary conditions are once again enforced such that the solvent can readily migrate throughout the domain. The results of this stage is shown in the last row.

Focusing now our attention on this last row, we can see at the end of the simulation that the disks formation stage has a drastic effect on the resulting sizes of the yellow domains as well as of their dispersity.

In particular, when the disks formation stage lasted for 10^9 iterations (third column), the final domains were significantly larger compared to the shorter disks formation stage (second column). Comparing the run without the disks formation stage to the middle one reveals less drastic changes in the end stage of the evolution, showing however clear differences in the initial stage, when there is significant amount of solvent in the system.

The disks formation stage was introduced as a way to generate the rubber balls added to the mixture in the experimental setup[8]; compare figure 1. With this in mind, and comparing the results obtained herein, we have opted to run the remaining simulations with 10^8 disks formation iterations as a compromise between omitting this stage and initializing with large yellow regions.

3.2. The effect of varying temperature

The next effect we have explored is that of varying the temperature in the system, i.e. changing the parameter β, directly proportional to the inverse temperature. Since we study a small section of a larger sample, the temperature within our domain will always be held constant. In the experimental setup, however, one often observes a temperature gradient; see [LPA+21] for

[8] This stage can potentially be developed further by embedding an optimization step to search for optimal rubber distributions. This is though out of the scope of the current work.

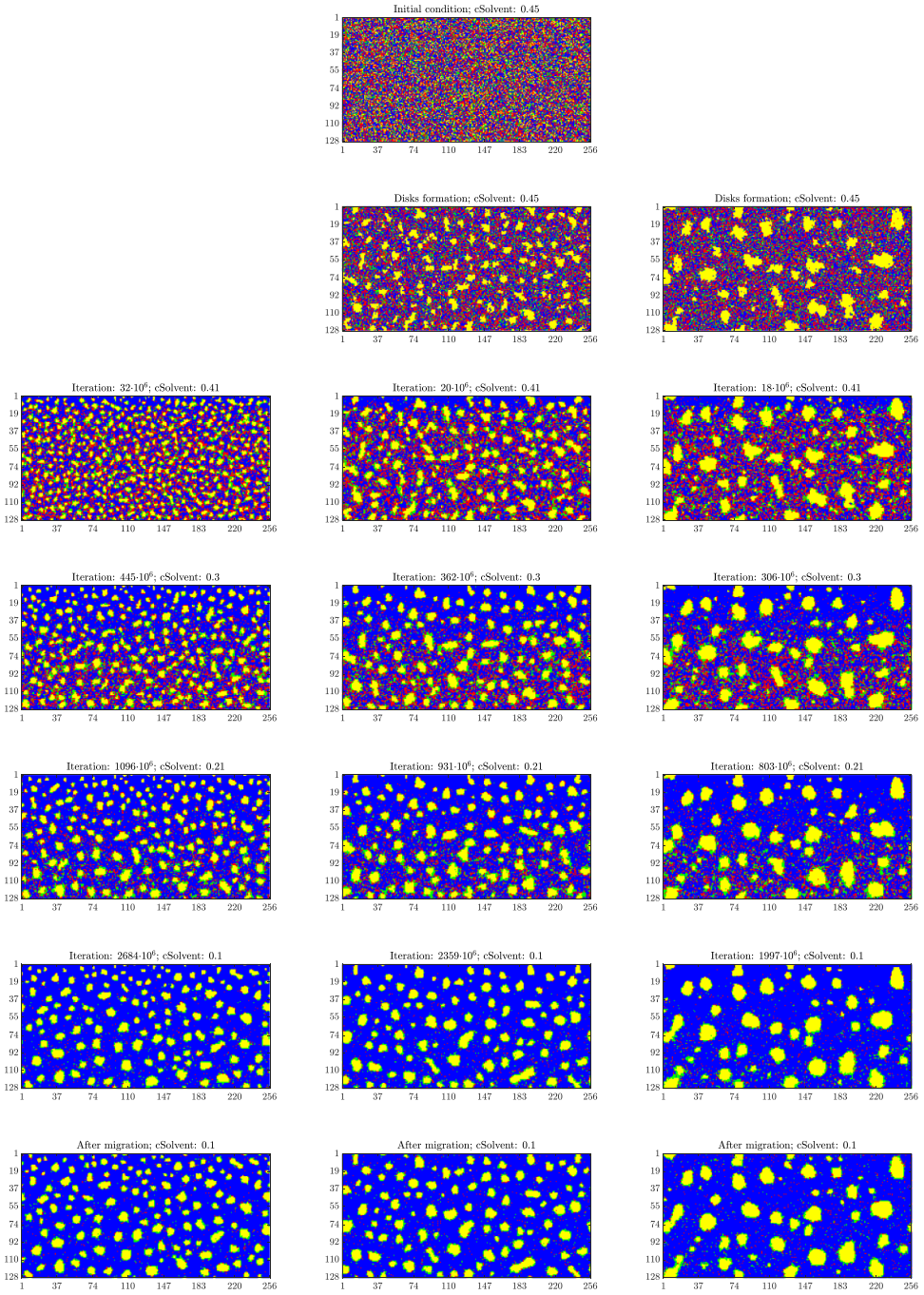

Figure 2. The effect of the disks formation stage at fixed temperature $\beta = 0.6$. Each simulation started with the common initial condition in the top middle frame. The disks formation stage was deactivated in the first column and activated for 10^8, respectively 10^9 iterations in the second and third columns (second row). The evaporation stage stopped at a combined solvents concentration of 0.1 (second to bottom row), and then the migration stage was switched on for 10^8 iterations (bottom row).

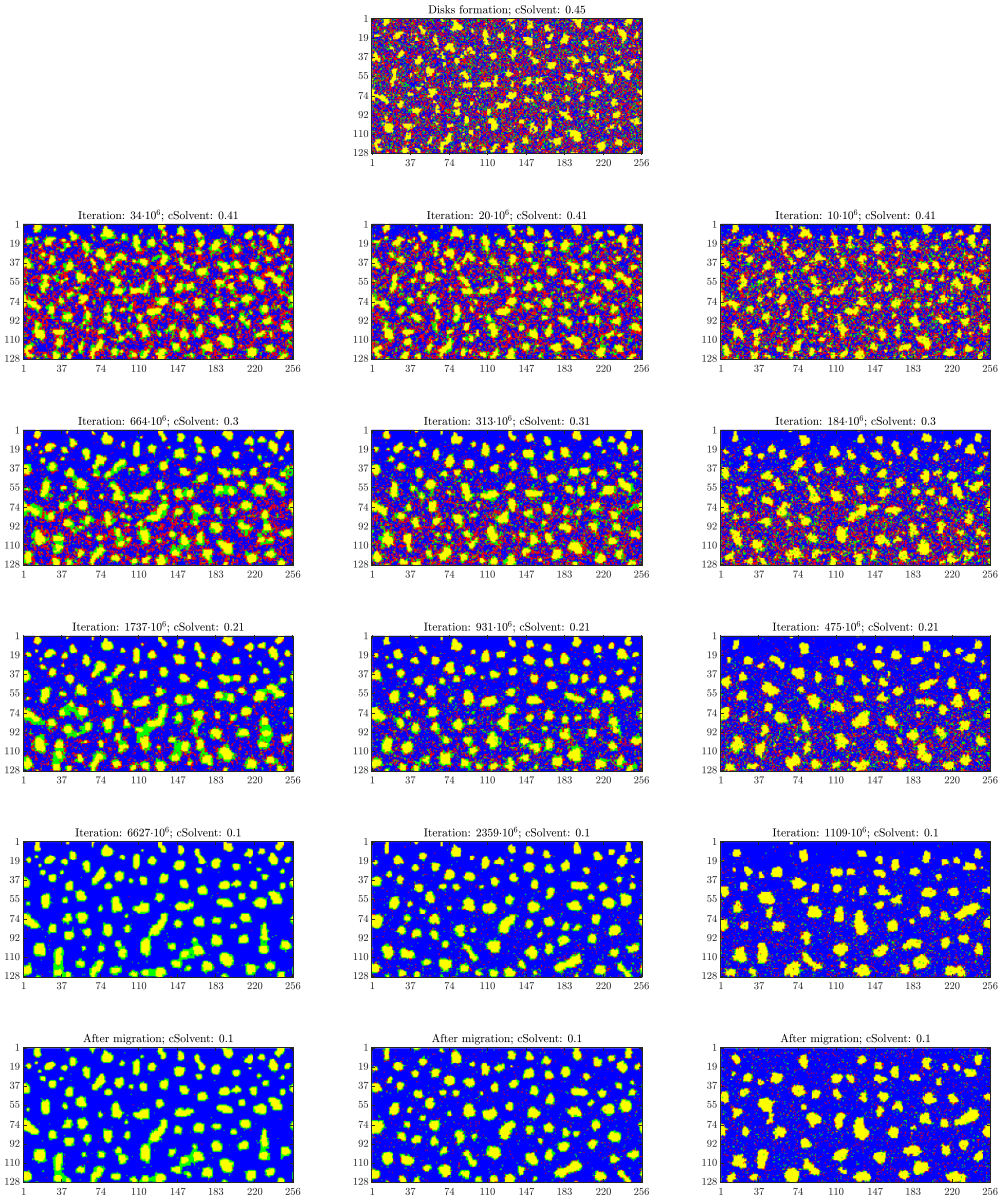

Figure 3. The effect of changing the temperature. Each simulation started with the common initial condition in the top middle frame, after the disks formation stage was activated for 10^8 iterations. The left, middle and right columns represent $\beta = 0.9$, 0.6 and 0.3, respectively. Note that increasing temperature is related to more domain growth and less condensation of the solvents.

a related setting. Whence, altering the temperature of our system could be viewed as observing different slices along the temperature gradient in the experimental setup.

The simulations are shown in figure 3, where the common initial configuration is shown in the top row. As before, successive rows show the systems at 10% reduction of solvent in the

system, and the dynamics are once more switched off at 10% remaining solvent (second to last row). This time, each column represents different temperatures, going from cold (first column; $\beta = 0.9$) to warm (third column; $\beta = 0.3$) with an intermediate temperature of $\beta = 0.6$ in the second column.

Increasing temperature does not seem to have a drastic effect on the domain growth, but it related to less condensation of the solvents. For example, in the first column (coldest system), the green solvent condenses around the rubber structures (yellow), and they stay condensed throughout the evolution of the system. Returning to the interaction matrix equation (2), this behavior is easily understandable, since this solvent is less repelled by the yellow sites compared to the blue ones. The low temperature means that non-energetically favorable movements are significantly less likely to occur, so that the condensate is stable.

In the second column, the green solvent still condenses around the yellow phase, but it does not produce 'solvent bridges' between isolated yellow regions, like in the coldest case. Instead, the yellow regions connected via such solvent bridges before, now often merge to one larger yellow structure.

Finally, for the warmest system in the third column, the green solvent no longer readily condenses around the yellow phase and instead evaporates together with the red solvent. Note that the red solvent evaporates more easily in general, since it is less repulsed by the blue phase, and hence is able to migrate to the top boundary, even at lower temperatures.

4. Conclusion and outlook

We conclude our work with a few thoughts what concern further possible investigations in the same direction, viz.

- The model captures the diffusion of the many components of the mixture, their interactions, as well as the evaporation mechanism of the solvents. The obtained morphologies are in the expected physical range.
- The interplay between the temperature and the two solvents is very complex. Interestingly, looking at figure 3, we can see that solvent 1 (the red solvent) can diffuse to the top boundary more easily, hence it can evaporate more rapidly. On the other hand, solvent 2 (the green solvent) tends to stay surrounding the rubber morphologies. If enough energy is available (i.e. at low values of β, associated with high temperatures), then also this solvent can diffuse to the top boundary and then evaporate.
- The disks formation phase and the migration (terminal) phase can potentially be used for the purpose of morphology design. This would natural involve not only a rather involved optimization step but also more information on the physics and chemistry of the involved components in the mixture.
- As further study, we think it is worth estimating numerically the coarsening rates of the rubber balls and seeing how do they depend on the solvent–solute interaction parameters. Such study would need to involve a careful quantitative analysis of the obtained morphologies in terms of correlation and structure factors calculations; the procedure set up in [MKC+22] can be adapted to be applicable to the scenario presented here.
- In future works, we will tackle the challenge to model the non-equilibrium process of evaporation differently than imposing the solvents to be in a perfect contact with an infinite reservoir. We would like to be able to describe variants of the Raoult and Henry's laws in terms of particles interacting together in a thin layer (with finite volume) placed on the top of the adhesive layer.

- Last, but not least, if we think of the practical problem where the produced morphologies of the adhesives must be sticky, we believe that either coupling our lattice model with a continuum-based description of the mechanics of the situation, or developing a multi-component Cahn–Hilliard-type system to be coupled with a mechanics model for the adhesive band would be of help for understanding better the role played by the shape and dispersivity of the microscopic rubber morphology in allowing the resulting material to undergo large macroscopic deformations.

Data availability statement

The data that support the findings of this study are openly available at the following URL/DOI: https://github.com/vcekron/solventAdhesive.

Acknowledgments

An initial formulation of the problem was posed as scientific challenge to MiMM Day® 2021 (Mathematics with Industry Day) by researchers from the company tesa SE (Germany). We thank our collaborators Professor E N M Cirillo (La Sapienza University, Rome, IT) and Dr M Colangeli (University of L'Aquila, IT) for what we have learnt from them during the years concerning lattice-based modeling and simulation. SAM acknowledges partial funding from the Swedish National Space Agency (Grant 174/19) and the Knut and Alice Wallenbergs Stiftelse (Grant 2016.0059) for her work on the modeling of morphology formation.

Appendix. Discussion of the parameter J_{22}

In this appendix, we discuss briefly the role of the attraction parameter J_{22} present in the interaction matrix J. A similar discussion can be made for the rest of the entries of J, combined eventually with explorations of parameter ranges for the initial volume fractions for each component of the mixture. We refer the reader to [CCM+19] for an investigation of this type for a three-component mixture, where one component is allowed to evaporate in the same as in this context. The concrete application we had in mind in [CCM+19] (and in the follow-up articles mentioned in the references section) was related to the issue of morphology formation for OSCs, a topic which share a number of conceptual similarities with the problem at hand—the formation of rubber disks-like morphologies as needed in the design of solvent borne adhesives.

In order to shed some light on the complexity of choosing an appropriate interaction matrix J, we include a small discussion and additional simulation where we vary J_{22}, i.e. the rubber–rubber (yellow–yellow) interaction. The results are shown in figure 4, where the simulations all started with the lattice in the top middle frame.

After the disks formation stage was activated for 10^8 iterations, the frames in the second row were observed. Here, we note that there are no domains formed in the first column, since $J_{22} = 0$, so that all elements in J are zero, and the only changes when compared to the initial frame come from thermal fluctuations. For $J_{22} = -4$ in the middle column, we see larger domains than when $J_{22} = -8$ in the last column. Since we are in some sense aiming to emulate the experimental observations in figure 1, the middle one seems preferable due to the relative sizes of the yellow (rubber) domains.

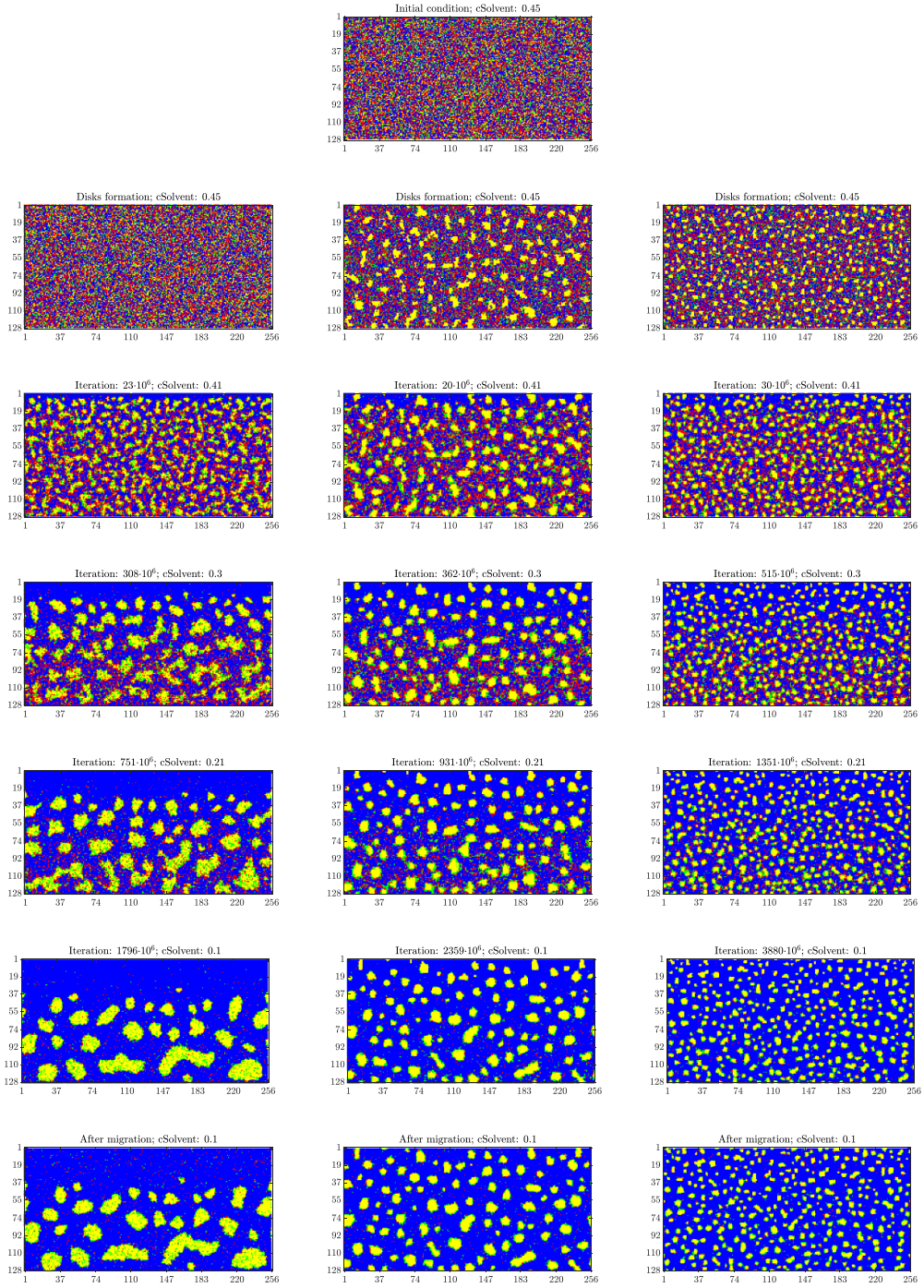

Figure 4. The effect of varying J_{22} from 0, -4, and -8 in the first, middle and last column, respectively ($\beta = 0.6$). Each simulation started with the common initial condition in the top middle frame. The disks formation stage was activated for 10^8 iterations, but since $J_{22} = 0$ in the first column, no domains were formed.

During the evaporation process, we see that the yellow domains grow significantly when $J_{22} = 0$. This leads to oddly-shaped yellow regions that dominate the lattice, and a large blue 'roof' on top. This is rather far from the experimental picture, in comparison to the middle column, where we recover more round yellow regions that are more similar to the experimental findings. In the third column, meanwhile, we recover smaller domains that do not grow significantly during the simulation. Additionally, notice that the number of iterations required to reach the stopping criterion of 10% remaining solvent significantly increases with decreasing J_{22}. This is simply due to the fact that it becomes more and more 'expensive' for a yellow site to not be surrounded by fellow yellow sites, so that the domains become more and more immovable and stable.

Summarizing, we see that as long as the rest of our interaction matrix remains unchanged, we have picked a relatively good value of J_{22} for our purposes. This is only one parameter out of 16, so exploring the full space of the parameters to find an optimal set is very difficult, especially when our reference for 'good results' is only qualitative.

ORCID iDs

V Cecilia Erik Kronberg https://orcid.org/0000-0001-6076-9119
Stela Andrea Muntean https://orcid.org/0000-0001-9337-2249
Nils Hendrik Kröger https://orcid.org/0000-0001-5336-4869
Adrian Muntean https://orcid.org/0000-0002-1160-0007

References

[CCM+19] Cirillo E N M, Colangeli M, Moons E, Muntean A, Muntean S A and van Stam J 2019 A lattice model approach to the morphology formation from ternary mixtures during the evaporation of one component *Eur. Phys. J. Spec. Top.* **228** 55–68

[CMv19] Cirillo E N M, Muntean A and van Santen R 2019 Particle–based modelling of flows through obstacles *Complexity Science: An Introduction* (World Scientific)

[EBS+20] Eumelen G J A M, Bosco E, Suiker A S J, Hermans J J, van Loon A, Keune K and Iedema P D 2020 Computational modelling of metal soap formation in historical oil paintings: the influence of fatty acid concentration and nucleus geometry on the induced chemo-mechanical damage *SN Appl. Sci.* **2** 1310

[Han70] Hansen C M 1970 Polymer coatings. Concepts of solvent evaporation phenomena *Ind. Eng. Chem. Prod. Res. Dev.* **9** 282–6

[LGLM99] Lee S, Goo J, Lee H and Mumby S J 1999 Molecular dynamics simulations of the enthalpy of mixing of poly(vinyl chloride) and aliphatic polyester blends *Polymer* **40** 5137–45

[LPA+21] Leguizamon S C, Powers J, Ahn J, Dickens S, Lee S and Jones B H 2021 Polymerization-induced phase separation in rubber-toughened amine-cured epoxy resins: tuning morphology from the nano- to macro-scale *Macromolecules* **54** 7796–807

[MGNR12] Müller-Gronbach T, Novak E and Ritter K 2012 *Monte Carlo-Algorithmen* (Springer)

[MKC+22] Muntean S A, Kronberg V C E, Colangeli M, Muntean A, van Stam J, Moons E and Cirillo E N M 2022 Quantitative analysis of phase formation and growth in ternary mixtures upon evaporation of one component *Phys. Rev.* E **106** 025306

[MMM21] Mapari S, Mestry S and Mhaske S T 2021 Developments in pressure-sensitive adhesives: a review *Polym. Bull.* **78** 4075–108

[OMIK99] Okabe Y, Miyajima T, Ito T and Kawakatsu T 1999 Application of Monte Carlo method to phase separation dynamics of complex systems *Int. J. Mod. Phys.* C **10** 1513–20

[RKZ+23] Roubicek T, Kruzik M, Zeman J, Panagiotopoulos C G, Vodicka R and Mantic V 2023 Delamination and adhesive contacts, their mathematical modeling and numerical treatment *Computational and Experimental Methods in Structures. Mathematical Methods and Models in Composites* vol 3 (World Scientific) ch 13, pp 497–578

[SEP+21] Silva L A, Espinosa C, Paroissien E, Lachaud F and da Silva M 2021 Numerical simulations of adhesive spreading during bonding-induced squeeze *J. Adhes.* **78** 4075–108

[SKM+23] Setta M, Kronberg V C E, Muntean S A, Moons E, van Stam J, Cirillo E N M, Colangeli M and Muntean A 2023 A mesoscopic lattice model for morphology formation in ternary mixtures with evaporation *Commun. Nonlinear Sci. Numer. Simul.* **119** 107083

[YHG+18] Ye L *et al* 2018 Quantitative relations between interaction parameter, miscibility and function in organic solar cells *Nat. Mater.* **17** 253–60